

A radial velocity survey of low Galactic latitude structures: III. The Monoceros Ring in front of the Carina and Andromeda galaxies

N. F. Martin^{1,2}, M. J. Irwin², R. A. Ibata¹, B. C. Conn³, G. F. Lewis³,
M. Bellazzini⁴, S. Chapman⁵ & N. Tanvir⁶

¹ *Observatoire de Strasbourg, 11, rue de l'Université, F-67000, Strasbourg, France*

² *Institute of Astronomy, Madingley Road, Cambridge, CB3 0HA, U.K.*

³ *Institute of Astronomy, School of Physics, A29, University of Sydney, NSW 2006, Australia*

⁴ *INAF - Osservatorio Astronomico di Bologna, Via Ranzani 1, 40127, Bologna, Italy*

⁵ *California Institute of Technology, Pasadena, CA, 91125, USA*

⁶ *Physical Sciences, Univ. of Hertfordshire, Hatfield, AL10 9AB, U.K.*

12 September 2018

ABSTRACT

As part of our radial velocity survey of low Galactic latitude structures that surround the Galactic disc, we report the detection of the so called Monoceros Ring in the foreground of the Carina dwarf galaxy at Galactic coordinates $(l, b) = (260^\circ, -22^\circ)$ based on VLT/FLAMES observations of the dwarf galaxy. At this location, 20 degrees in longitude greater than previous detections, the Ring has a mean radial velocity of $145 \pm 5 \text{ km s}^{-1}$ and a velocity dispersion of only $17 \pm 5 \text{ km s}^{-1}$. Based on Keck/DEIMOS observations, we also determine that the Ring has a mean radial velocity of $-75 \pm 4 \text{ km s}^{-1}$ in the foreground of the Andromeda galaxy at $(l, b) \sim (122^\circ, -22^\circ)$, along with a velocity dispersion of $26 \pm 3 \text{ km s}^{-1}$. These two kinematic detections are both highly compatible with known characteristics of the structure and, along with previous detections provide radial velocity values of the Ring over the $120^\circ < l < 260^\circ$ range. This should add strong constraints on numerical models of the accretion of the dwarf galaxy that is believed to be the progenitor of the Ring.

Key words: Galaxy: structure – galaxies: interactions – Galaxy: formation

1 INTRODUCTION

With the public release of all sky surveys, many details have been gained in the structure of the outer parts of the Galactic disc. In particular, the Sloan Digital Sky Survey (SDSS) revealed the existence of a stellar structure in the anticentre direction, near the Galactic plane and slightly over the edge of the disc (Newberg et al. 2002). Visible as a clear main sequence at a Galactocentric distance of 18 kpc for $180^\circ < l < 225^\circ$ and $|b| < 30^\circ$, this structure is unlike what is expected for the Galactic disc. Ibata et al. (2003) used the INT Wide Field Camera to show this structure is in fact present in the second and third Galactic quadrants, circling the disc in a ring-like fashion. Radial velocity measurements also revealed a kinematically cold population with a velocity dispersion of only $15 - 25 \text{ km s}^{-1}$, once more unexpected for a Galactic structure, leading to the conclusion that this so-

called Ring¹ is produced by the accretion of a dwarf galaxy in the Galactic plane whose tidal arms are wrapped around the Milky Way.

Subsequently, much work has been invested in trying to determine the true extent of this Ring and where possible determine its kinematics to constrain the orbit of its progenitor. Rocha-Pinto et al. (2003) used the 2MASS catalogue to probe the distribution of M giant stars and found that the Ring may extend over the $120^\circ \lesssim l \lesssim 270^\circ$ range in the Northern hemisphere and be present in the Southern hemisphere, with $|b| < 35^\circ$. Conn et al. (2005a) extended the Ibata et al. (2003) INT/WFC survey to show the Ring is present within 30 degrees of the Galactic plane throughout the whole second quadrant but seems to disappear at $l \sim 90^\circ$. More constraints on the structure were gained

¹ This structure has been called many names including the Monoceros Ring, the Galactic Anticentre Stellar Structure or GASS and the Ring. Given its extent in Galactic longitude and its presence in numerous constellations, we prefer to call it simply the Ring.

by the Crane et al. (2003) spectroscopic survey of putative Ring M-giant stars in the anticentre direction ($150^\circ < l < 230^\circ$, $|b| < 40^\circ$) which confirmed that most of these stars are indeed linked to this structure. Using the simple model of a population orbiting the Milky Way in a prograde, circular orbit, they determined their sample was best fitted by a population at a Galactocentric distance of 18 kpc and with a rotational velocity of 220 km s^{-1} . The resulting velocity dispersion of $20 \pm 4 \text{ km s}^{-1}$ around this model is in good agreement with the velocity dispersion measured by the SDSS team (Yanny et al. 2003).

While tracking the Ring, two other structures were discovered that do not seem to be directly related to the Monoceros Ring. Using the 2MASS catalogue, Rocha-Pinto et al. (2004) reported the existence of a diffuse population of M giants in the direction of the Triangulum and Andromeda constellations, behind known detections of the Ring. Also using the 2MASS catalogue, our group presented evidence of a dwarf galaxy located closer than the Ring, just at the edge of the Galactic disc, in the Canis Major constellation (Martin et al. 2004; Bellazzini et al. 2004). In particular, we argued that the accretion of the Canis Major galaxy onto the Galactic disc would naturally reproduce similar features as the one observed for the Ring. However, a link between these three structures remains putative at the moment, even though current models show such a scenario is highly plausible (Peñarrubia et al. 2005; Martin et al. 2005; Dinescu et al. 2005).

To gain more insight into the nature of these structures, we have started a radial velocity survey of regions at low Galactic latitude where the Ring structure may be located. Using the AAT/2dF multi-fibre spectrograph, we first targeted the Canis Major dwarf (Martin et al. 2005). This survey also revealed the presence of the Ring behind the dwarf, with a Heliocentric radial velocity of $133 \pm 1 \text{ km s}^{-1}$ and dispersion of $23 \pm 2 \text{ km s}^{-1}$ at a Galactocentric distance of 19 kpc, highly compatible with previous detections (Conn et al. 2005b). In this third paper of the series, we report the presence of the Ring in the foreground of the Carina dwarf galaxy from VLT/FLAMES observations of the dwarf at $(l, b) = (260^\circ, -22^\circ)$. Using Keck2/DEIMOS observations of regions around M31, we also determine the radial velocity of the Ring at $(l, b) \sim (122^\circ, -22^\circ)$ where the Ring is known to exist but where its radial velocity has not yet been measured. Section 2 presents the Ring detection in front of Carina and Section 3 deals with the detection in front of the Andromeda galaxy. Section 4 concludes this letter.

In the following, all the magnitudes have been corrected for extinction using the maps from Schlegel, Finkbeiner & Davis (1998). We also assume that the Solar radius is $R_\odot = 8 \text{ kpc}$, that the LSR circular velocity is 220 km s^{-1} , and that the peculiar motion of the Sun is ($U_0 = 10.00 \text{ km s}^{-1}$, $V_0 = 5.25 \text{ km s}^{-1}$, $W_0 = 7.17 \text{ km s}^{-1}$; Dehnen & Binney 1998). Except when stated otherwise, the radial velocities, v_r , are Heliocentric radial velocities, not corrected for the motion of the Sun.

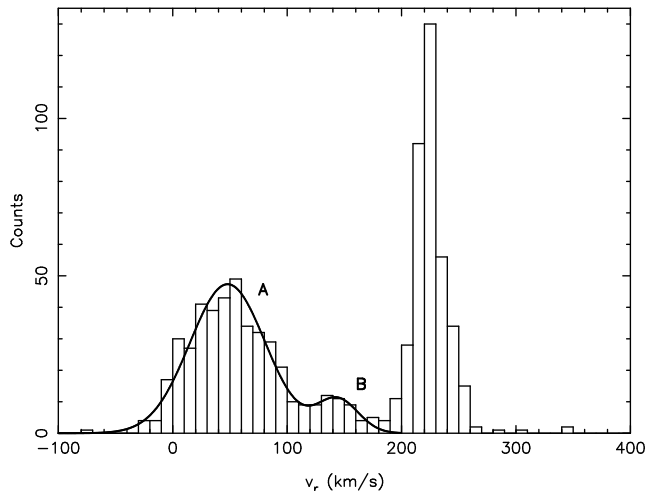


Figure 1. Velocity distribution of the FLAMES sample. The peak at $v_r \sim 220 \text{ km s}^{-1}$ is produced by Carina stars. Stars with $v_r < 180 \text{ km s}^{-1}$ are well fitted by a double Gaussian model (represented by the black thick line) with populations A and B centred on 49 ± 7 and $145 \pm 5 \text{ km s}^{-1}$ and with dispersions of 33 ± 2 and $17 \pm 5 \text{ km s}^{-1}$ respectively.

2 THE RING IN FRONT OF THE CARINA DWARF GALAXY

FLAMES observations in the Carina fields were taken from the public access ESO raw data archive² and included 14 setups centred on various fields designed to study the Carina dwarf galaxy. The total integration time of each setup was typically 15000 seconds giving excellent signal-to-noise ($>20:1$ per 0.2 \AA sampling element) for the Galactic foreground stars in these directions. The Carina data plus calibration sequences were downloaded and processed through the standard ESO FLAMES low resolution pipeline.

At the time of using the pipeline, sky subtraction was not part of the pipeline procedure so the remaining processing steps used the FLAMES software developed for the DART project (see e.g. Tolstoy et al. 2004). Briefly, this software stacks the individual repeat spectra on the same target field; combines all the sky observations to form a master sky spectrum; and then optimally scales, shifts (if necessary) and resolution-matches the sky to the object spectrum prior to sky subtraction. The sky-subtracted spectra are then searched for CaII near infrared triplet lines and a model template CaII spectrum is used to extract velocity information.

The direct imaging used here also came from the ESO archive and comprised 4 V, I sequences of ESO/WFI data covering $\approx 1 \times 1$ square degrees centred on the Carina dwarf. This was processed through the standard Cambridge pipeline (Irwin & Lewis 2001) to produce catalogues of magnitudes, colours and object morphological classifications.

The velocity distribution of all the stars targeted with FLAMES is displayed on Figure 1. The most prominent feature is of course the peak of stars at $v_r \sim 220 \text{ km s}^{-1}$ produced by Red Giant Branch stars belonging to the Carina

² <http://www.eso.org/archive>

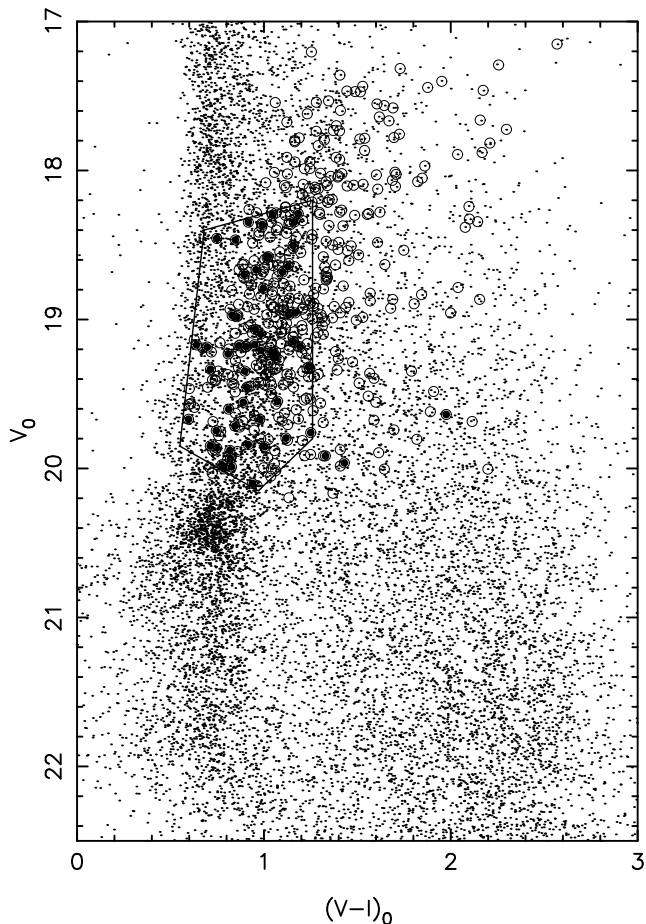


Figure 2. ESO/WFI Colour-Magnitude Diagram of the Carina region. Red Clump stars from the dwarf produce the feature around $V_0 \sim 20.5$ and $(V - I)_0 \sim 0.7$. DEIMOS target stars, that were chosen along the dwarf’s red giant branch, are highlighted with those that show a radial velocity under 110 km s^{-1} plotted as hollow circles (population A) while stars with $110 < v_r < 180 \text{ km s}^{-1}$ are shown as filled circles (population B). The two populations show highly dissimilar behaviours, with almost all population B stars bluer than $(V - I)_0 = 1.3$. The selection box that is used for comparison with the Besançon model is also shown.

dwarf galaxy (the primary targets of these FLAMES observations). Stars with $v_r < 180 \text{ km s}^{-1}$ are expected to be Galactic stars belonging to the thin disc, thick disc and/or stellar halo. However, they seem to follow a bimodal Gaussian distribution produced by populations with central velocities and dispersions of $(\mu_A, \sigma_A) = (49 \pm 7 \text{ km s}^{-1}, 33 \pm 2 \text{ km s}^{-1})$ and $(\mu_B, \sigma_B) = (145 \pm 5 \text{ km s}^{-1}, 17 \pm 5 \text{ km s}^{-1})$ and a 9 to 1 ratio according to a maximum likelihood fit of a two component Gaussian model. Although population A has the expected characteristics of a disc-like population in the foreground, the low dispersion of population B is more puzzling.

The Colour-Magnitude Diagram (CMD) of Figure 2 displays the location of stars belonging to these two populations with hollow circles for population A stars ($v_r < 110 \text{ km s}^{-1}$) and filled circles for population B stars ($110 < v_r < 180 \text{ km s}^{-1}$). The two populations show drastically different

colour-magnitude distributions, pointing at a genuine difference between them. Population A is widely spread in colour and follows, once more, the expected distribution of foreground disc stars. On the other hand population B is confined on the bluer part of our sample, with almost all stars having $(V - I)_0 < 1.3$. Of the three stars with $(V - I)_0 > 1.3$, the one with the highest $(V - I)_0$ is only just a population B star with $v_r = 112 \text{ km s}^{-1}$ (the two others have radial velocities of 143 and 149 km s^{-1}).

Such a sharp colour cut makes it very unlikely that population B is produced by disc stars. Among the Galactic components, only the stellar halo is expected to have such behaviour (see e.g. Conn et al. 2005a for a comparison of the disc and halo Galactic component CMDs as they appear in the Besançon model of Robin et al. 2003). However, the velocity dispersion of the halo is $\sim 100 \text{ km s}^{-1}$ (e.g. Gould 2003), at odds with the 17 km s^{-1} found for population B. Since this low dispersion could be an artifact of the radial velocity cuts we used, we investigate the number of stars that would be expected for a halo population at $(l, b) = (260^\circ, -22^\circ)$. According to the synthetic Besançon model of Galactic stellar populations (Robin et al. 2003), there should be less than 225 halo stars per square degree in the CMD region highlighted on Figure 2 and that contains most of our population B stars, independently of radial velocity. Since our FLAMES targets roughly cover 0.25 square degrees, we would expect our sample to contain less than 60 halo stars if complete. Assuming the Milky Way is surrounded by a non-rotating stellar halo with a velocity dispersion of 100 km s^{-1} , our sample should contain only ~ 15 halo stars within $110 \text{ km s}^{-1} < v_r < 180 \text{ km s}^{-1}$, once again, if it were complete. Since within the selection box of Figure 2, the completeness is under 5%, it is highly unlikely that the 56 population B stars belong to the halo. Therefore, population B is most likely a non-Galactic population of stars that lie in front of the Carina dwarf galaxy, with a mean radial velocity of $145 \pm 5 \text{ km s}^{-1}$ and a velocity dispersion of $17 \pm 5 \text{ km s}^{-1}$.

A direct comparison with the velocity distribution of all the stars from the model that fall in the same region of the CMD would of course be more suited for our purpose. However the model greatly overpredicts the number of thick disc stars in this region of the sky when compared to the observations. This is probably due to an overestimate of the thick disc flare in the model. Although population A is very well reproduced by the thin disc population of the model, the modeled thick disc population is twice as numerous, centred on $v_r \sim 80 \text{ km s}^{-1}$ and with a high dispersion of $\sim 50 \text{ km s}^{-1}$. Such a population is clearly not present in our data. Since the sharp $(V - I)_0 < 1.3$ colour limit of population B is not expected for a disc population, we prefer comparing population B with only the halo population of the model.

With a detection of the Ring behind the Canis Major galaxy under the Galactic disc only 20 degrees away in Galactic longitude from the feature we detect in front of Carina, this population could be another detection of the Ring. Previous detections of the Ring have mainly relied on CMDs and especially on the main sequence of this population compared to the disc population at brighter magnitudes (Newberg et al. 2002; Ibata et al. 2003; Conn et al. 2005a). Unfortunately, for the Carina CMD, the red clump

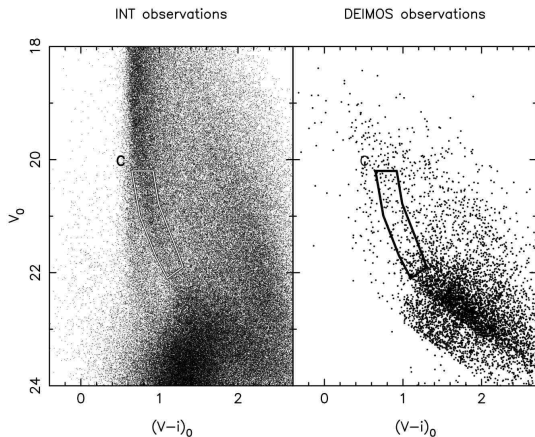


Figure 3. Colour-Magnitude Diagram of the INT ‘M31-N’ field of Ibata et al. (2003) (left panel) and the corresponding stars targeted with DEIMOS (right panel). The clear main sequence of the INT CMD is used to define a selection box of Ring stars (labeled C).

of the dwarf galaxy at $(V - I)_0 \sim 0.7$ and $V_0 \sim 20.5$ lies in the region of interest for detecting the Ring main sequence. However, comparison with fiducials shows the location of population B stars is not incompatible with turn-off stars from the old metal-rich population at a Galactocentric distance of ~ 20 kpc that is usually assumed for the Ring; even though the Carina-driven selection criteria applied to select the stars in the sample prevents a reliable comparison.

The radial velocity characteristics of this population in front of Carina further supports a connection with the Ring. Indeed, the determined velocity dispersion of $17 \pm 5 \text{ km s}^{-1}$ is within the $15 - 25 \text{ km s}^{-1}$ range of the SDSS and Crane et al. (2003) detections and close to the $24 \pm 2 \text{ km s}^{-1}$ of the detection in the background of Canis Major. For this latter case, the higher uncertainties on the 2dF radial velocity value of each star ($\sim 10 \text{ km s}^{-1}$) compared to those of the FLAMES derived velocities ($\sim 3 \text{ km s}^{-1}$) may also artificially increase the dispersion. When corrected from the Solar motion, the mean radial velocity of population B, $v_{\text{gsr},B} = -65 \text{ km s}^{-1}$, is very close to the $v_{\text{gsr},\text{bCMa}} = -67 \text{ km s}^{-1}$ found only 20 degrees away behind the Canis Major dwarf galaxy.

Therefore, we conclude that the non-Galactic population we have uncovered in front of the Carina dwarf galaxy is most likely part of the Ring.

3 KINEMATICS OF THE RING IN FRONT OF THE ANDROMEDA GALAXY

The presence of the Ring in front of the Andromeda galaxy was first reported by Ibata et al. (2003) from the analysis of INT/WFC Colour-Magnitude diagrams. The CMD of their ‘M31-N’ field is shown on the left panel of Figure 3 and the Ring is clearly visible as a main sequence that extends from $(V - i, V)_0 \sim (1.2, 22)$ to $(V - i, V)_0 \sim (0.6, 20.0)$. During our Keck/DEIMOS survey of M31 outer disc and halo substructures (e.g. Ibata et al. 2005), we took the opportunity to target foreground Ring stars that fortuitously

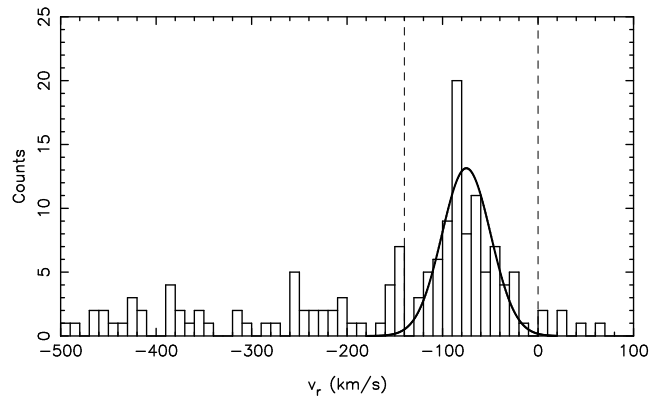


Figure 4. Radial velocity distribution of DEIMOS stars that fall in the Ring selection box (labeled C in Figure 3). The few stars with $v_r \sim -200 \text{ km s}^{-1}$ may contain M31 disc stars (the primary targets of these observations). Observed stars with $-140 \text{ km s}^{-1} < v_r < 0 \text{ km s}^{-1}$ (within the two dashed lines) are well fitted by a Gaussian model with a mean velocity of $-75 \pm 4 \text{ km s}^{-1}$ and a dispersion of $26 \pm 3 \text{ km s}^{-1}$ (represented by the black thick line).

fall in the targeted regions. The data were reduced as in Ibata et al. (2005) and the CMD of all the stars with a radial velocity uncertainty lower than 10 km s^{-1} is presented on the right panel of Figure 3. To select only probable members of the Ring structure, we construct a selection box around the Ring main sequence from the INT CMD (box C in Figure 3). Among the stars in the DEIMOS sample, 86 fall within this Ring selection box and the radial velocity distribution of these stars is displayed on Figure 4. Aside from Galactic halo and M31 disc stars at $v_r < -200 \text{ km s}^{-1}$, a peak is apparent at $\sim -70 \text{ km s}^{-1}$. Applying a maximum likelihood algorithm to fit with a Gaussian model those stars with $-140 < v_r < 0 \text{ km s}^{-1}$ that produce the peak, reveals that this population has a mean velocity of $-75 \pm 4 \text{ km s}^{-1}$ and an intrinsic dispersion of $26 \pm 3 \text{ km s}^{-1}$, corrected for the uncertainties on each measured radial velocity.

A direct comparison with the radial velocity distribution of stars from the Besançon model within the same sky region ($119^\circ < l < 124^\circ$ and $-24^\circ < b < -19^\circ$) and that fall in the same CMD selection box reveals the Ring sub-sample is not incompatible with the model. Indeed, a Kilmogorov-Smirnov test yields a probability of 10 percent that the two populations are identical. However, it is not unexpected that disc stars and Ring stars should show similar behaviour since both populations are believed to orbit the Milky Way on nearly circular orbits and the small shift in distance between them does not translate into a significant difference in radial velocity. Given that our selection box is constructed to contain Ring stars, it would be surprising that all the stars of the sample belong to the Galactic disc. On the contrary, we find it more likely that we are observing mainly Ring stars, as is suggested by the relatively low velocity dispersion of $26 \pm 3 \text{ km s}^{-1}$ in the sample, at odds with the $\sim 50 \text{ km s}^{-1}$ found in the Besançon model within the selection box. This low dispersion is also compatible with previous detections, especially since some disc and/or halo stars certainly fall in the same radial velocity range and increase the dispersion. The mean Heliocentric velocity of $-75 \pm 4 \text{ km s}^{-1}$ which converts to a Galactocentric standard of rest radial velocity of

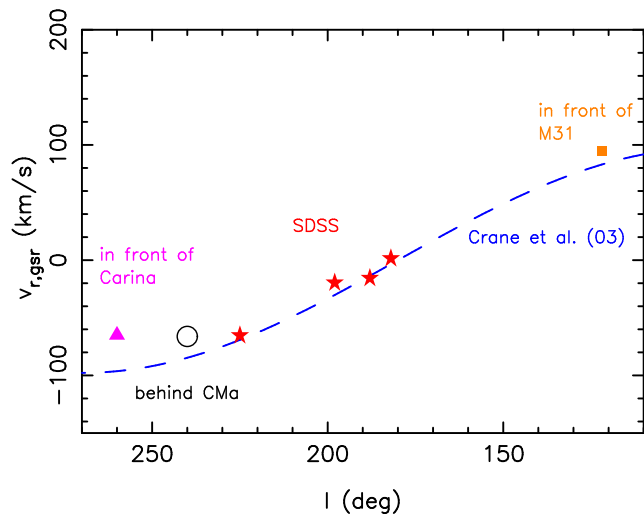


Figure 5. Summary of all known radial velocity detections of the Ring in the Galactic standard of rest. The dashed line corresponds to the Crane et al. (2003) model of the Ring: a population orbiting the Milky Way at a Galactocentric distance of 18 kpc and with a rotational velocity of 220 km s^{-1} . The Yanny et al. (2003) SDSS detections are shown as stars, the Conn et al. (2005b) detection behind Canis Major is shown by a hollow circle and the two detections of this letter in front of Carina and M31 are shown as a filled triangle and a filled square respectively. Uncertainties on these values are not shown since they are smaller than the used symbols. Though near the Crane et al. (2003) model, detections away from the anticentre tend to be offset from the model.

$v_{\text{gsr}} = 94 \pm 4 \text{ km s}^{-1}$ is also only slightly higher than the simple circular Crane et al. (2003) model. As for the detection in the foreground of the Carina dwarf, the radial velocity similarities between the previous detections of the Ring and the population in front of M31 strengthen the Ring nature of our detection.

4 SUMMARY AND CONCLUSION

We have presented the detection of two groups of stars that lie in front of the Carina dwarf galaxy at $(l, b) = (260^\circ, -22^\circ)$ and in front of the Andromeda galaxy at $(l, b) \sim (122^\circ, -22^\circ)$ and that cannot be satisfyingly explained by known Galactic components. The proximity with known detections of the Ring that surrounds the Galactic disc makes it highly probable that they belong to the same structure. Both detections have a low velocity dispersion ($17 \pm 5 \text{ km s}^{-1}$ and $26 \pm 3 \text{ km s}^{-1}$ respectively), a characteristic value encountered in all previous detections of the Ring.

With the Ring detection behind the Canis Major dwarf galaxy reported by Conn et al. (2005b), the radial velocity of the Ring population is now sampled throughout the $120^\circ < l < 260^\circ$ range, which should provide important constraints on N-body models. However, it can be directly seen in Figure 5 that currently known radial velocity values for the Ring are not exactly reproducible by the Crane et al. (2003) simple circular model. In fact, trying to fit all the detections in a single orbit of the progenitor proves unsatisfactory, whether the orbit is forced to be circular or allowed

to be slightly elliptical. It would therefore seem that models where the Ring completely surrounds the Galactic disc with multiple tidal arms are following the right track (see e.g. Peñarrubia et al. 2005 and Martin et al. 2005). In addition to the new radial velocities we report in this letter, such models would highly benefit from a similar survey as the one presented in Conn et al. (2005a), but this time to higher longitudes to study in more detail the morphology of the Ring in these regions and especially to add a distance constraint to the detection in front of the Carina dwarf.

ACKNOWLEDGEMENTS

NFM is grateful to the IoA for the kind hospitality during the months at Cambridge in which this work was mainly performed. NFM acknowledges support from a Marie Curie Stage Research Training Fellowship under contract MEST-CT-2004-504604. GFL acknowledges support from ARC DP 0343508 and is grateful to the Australian Academy of Science for financially supporting a collaborative visit to Strasbourg Observatory.

REFERENCES

- Bellazzini M., Ibata R. A., Monaco L., Martin N. F., Irwin M. J. & Lewis G. F. 2004, MNRAS 354, 1263
 Conn B., Lewis G., Irwin M., Ibata R., Irwin J., Ferguson A. & Tanvir N. 2005a, MNRAS 362, 475
 Conn B., Martin N., Lewis G., Ibata R., Bellazzini M. & Irwin M. 2005b, MNRAS 364L, 13
 Crane J., Majewski S., Rocha-Pinto H., Frinchaboy P., Skrutskie M. & Law D. 2003, ApJ 594, L119
 Dehnen W. & Binney J. 1998, MNRAS 298, 387
 Dinescu D., Martínez-Delgado D., Girard T., Peñarrubia J., Rix H.-W., Butler D. & van Altena W. 2005, ApJ 631, L49
 Gould A. 2003, ApJ 583, 765
 Ibata R., Irwin M., Lewis G., Ferguson A. & Tanvir N. 2003, MNRAS 340, 21
 Ibata R., Chapman S., Ferguson A. M. N., Lewis G., Irwin M. & Tanvir N. 2005, ApJ 634, 287
 Irwin M. & Lewis J. 2001, NewAR 15, 105
 Martin N., Ibata R., Bellazzini M., Irwin M., Lewis G. & Dehnen W. 2004, MNRAS 348, 12
 Martin N., Ibata R., Conn B., Lewis G., Bellazzini M. & Irwin M. 2005, MNRAS 362, 906
 Newberg H. et al. 2002, ApJ 569, 245
 Peñarrubia J., Martínez-Delgado D., Rix H.-W., Gómez-Flechoso M. A., Munn J., Newberg H., Bell E. F., Yanny B., Zucker D. & Grebel E. K. 2005, ApJ 626, 128
 Robin A., Reylé C., Derrière S. & Picaud S. 2003, A&A 409, 523
 Rocha-Pinto H., Majewski S., Skrutskie M. & Crane J. 2003, ApJ 594, L115
 Rocha-Pinto H., Majewski S., Skrutskie M., Crane J. & Patterson R. 2004, ApJ 615, 732
 Schlegel D., Finkbeiner D. & Davis M. 1998, ApJ 500, 525
 Tolstoy E. et al. 2004, ApJ 617L, 119
 Yanny B. et al. 2003, ApJ 588, 824